MIXED MODE FRACTURE MODELING OF CONCRETE USING A MODIFIED COULOMB'S LAW

Luciani N. Lens[a], Eduardo Bittencourt[b], Virgínia M. R. d'Avila[b]

[a] *Centro de Ciências Exatas e Tecnológicas, Universidade Estadual do Oeste do Paraná, Campus de Cascavel, Rua Universitária 2069, Cascavel, PR, Brazil,* lnlens@unioeste.br, *http://www.unioeste.br*
[b] *Centro de Mecânica Aplicada e Computacional, Univesidade Federal do Rio Grande do Sul, Avenida Osvaldo Aranha, 99, Porto Alegre, RS, Brazil,* bittenco@cpgec.ufrgs.br, *http://www.ppgec.ufrgs.br/Cemacom*

Keywords: Fracture Mechanics, concrete, cohesive surfaces, finite elements, mixed mode.

Abstract. A 2D model for plain concrete that considers discrete cracks is here proposed. Zero thickness cohesive surface elements are introduced between all adjacent finite elements. Mixed-mode rupture can be captured using a modified Coulomb's law. The classical zero thickness cohesive model was here modified in order to partially eliminate mesh dependency.

In this work, some well-known Mode I post-peak constitutive equations used in discrete fracture methodologies for concrete, are implemented in the cohesive surface method. The shape of these equations changes overall results and is linked with the development of the process zone. Pre-peak of the equations was modified in order to reduce mesh dependency. On the other side, Mode II constitutive equations and properties are not well known or defined in general. This issue is addressed here and a modified Coulomb's law is proposed to deal with mixed mode cases. The methodology is simple and, besides pure Mode I fracture properties, requires only the definition of a coupling factor between Mode I and II. An elastic-predictor and plastic-correct type of algorithm is used to define cohesive surface tractions. Results presented here are only preliminary but show that the methodology is able to capture correctly crack morphology as well as peak load in a simple 4 point double notched beam.

1   INTRODUCTION

One of the most used methods in recent past to simulate concrete rupture is the smeared method (Rashid, 1968; Cedolin and Dei Poli, 1977; Bazant and Cedolin, 1979, Rots and Blaauwendraad, 1989; Oliver, 1989; etc), where damage caused by fracture is considered only in the volumetric constitutive law of the material. Although overall results are satisfactory, cracks are not explicitly considered. The so-called embedded methods introduce cracks as a discontinuity of strains or displacements and are a closer representations of the real discontinuity (Grootenboer et al., 1981; Ortiz et al., 1987; Belytschko et al., 1988; Dvorkin et al., 1990, Dominguez et al., 2004, Brisotto et al. 2008, etc.). However, they are also approximations because the crack tip (and corresponding stress/strain field) is not considered. These methods in general work better in reinforced concrete, where, in most of the cases, there is not a predominant crack and the cracking phenomena can be considered a volumetric damage.

Fracture of plain concrete, where dominant cracks normally emerge, is better approximated by discrete methods in general, such as the adaptive methods (Wawrzynek and Ingraffea, 1987, Potyondy et al., 1995, etc.) and cohesive surface methods (Xu and Needleman, 1994, Camacho and Ortiz, 1996, etc.). In the first, a new crack surface is added to the boundary representation, when maximal stress exceeds a limit. The method requires that a fully new mesh be created in this case. In the second, cohesive surfaces are placed between all finite elements. When maximal traction at the surface exceed a limit, a new crack surface is then created by separation of finite element nodes. The method is obviously simpler, but may induce a mesh dependency on results. Recently, the so called X-FEM or extended finite element method by Belytschko et al. (1999, 2001), which is an adaptive methods that insert cohesive elements as the crack travels, was proposed as an alternative.

The constitutive model for the cohesive surface is represented by a function of the tractions in terms of separation distances between finite element faces, which corresponds to crack opening (Hillerborg et al., 1976, CEB-FIP Model Code, 1993 and Xu, 1999, etc.). Due to the process zone, constitutive model for concrete in Mode I presents a softening curve after traction strength is reached.

Considering mixed mode (I and II) fracture, Bocca et al. (1990), Cervenka (1994) and Gálvez et al. (2002) concluded that Mode II properties have little influence on results, suggesting that crack propagation is predominantly Mode I propagation, even when a global mixed mode loading is applied. Jenq and Shah (1988), García et al. (2000) and Di Prisco et al. (2000) also share the idea that Mode II is not an important fracture mechanism in concrete. Other studies indicate that Mode II energy is much higher than Mode I (Bažant and Pfeiffer, 1985, Rots, 1988 and Swartz et al., 1988). A physical explanation for an increase in Mode II energy comes from aggregate action (friction, interlock action, etc.) that practically eliminates the possibility of sliding inside the concrete. The increase found by Carpinteri et al. (1993) for Mode II energy was more modest than others, from 16 to 33% greater than Mode I energy. Actually they believe that Mode II energy is not a property in concrete and depends on the loading, shape and size of the body.

Even considering that rupture in Mode II is locally not feasable, interactions between normal and tangential tractions must be considered. In this work a cracking surface was created in order to define the combination of both during cracking. The surface chosen was a modified Coulomb law, where strength in tension is considered an adhesion. Besides Mode I properties, shear strength and an effective opening must be defined. However, numerical experimentation has shown that the last two properties have only a marginal effect on results.

It will be seen that this approach can be considered as a lower-bound for the cracking surface. Works that consider a coupling only through an effective opening, as in Basche et al. (2007), can be considered an upper-bound for the cracking surface. Constitutive laws used in this work for Mode I are presented and described in section 2; mixed mode considerations are made in section 3; section 4 shows applications of the methodology for four-points bending, mixed mode propagation. Concluding remarks and discussions are done in section 5. Implementation in a finite element (FE) context framework is described in Lens et al. (2007).

2   CONSTITUTIVE LAW FOR MODE I

To represent crack behavior is necessary to establish a relationship between normal traction (σ) and normal opening (w) of the surfaces. It is known that when surfaces start to separate from each other, traction increases reaching a peak value (σ_{max}). Afterwards, traction decreases until reach a zero value for crescent opening. For this opening, the surfaces are considered fractured. This behavior occurs in different scales, from separation of atomic planes to macro-scale at the crack tips. Depending on the scale or on the material being represented by separation of the surfaces, different peak tractions and final openings are used. A vast collection of such values can be found in Chandra et al. (2002). In the case of concrete, the constitutive law of cohesive surfaces is separated in two parts: the post-peak and the pre-peak parts as follows.

2.1 Post-peak of the Constitutive Law

Three shapes of post-peak constitutive laws are represented below: Hillerborg et al. (1976), CEB-FIP Model Code (1993) and Xu (1999). These relationships are implemented in the present work in the cohesive surface context and are depicted in Figure 1.
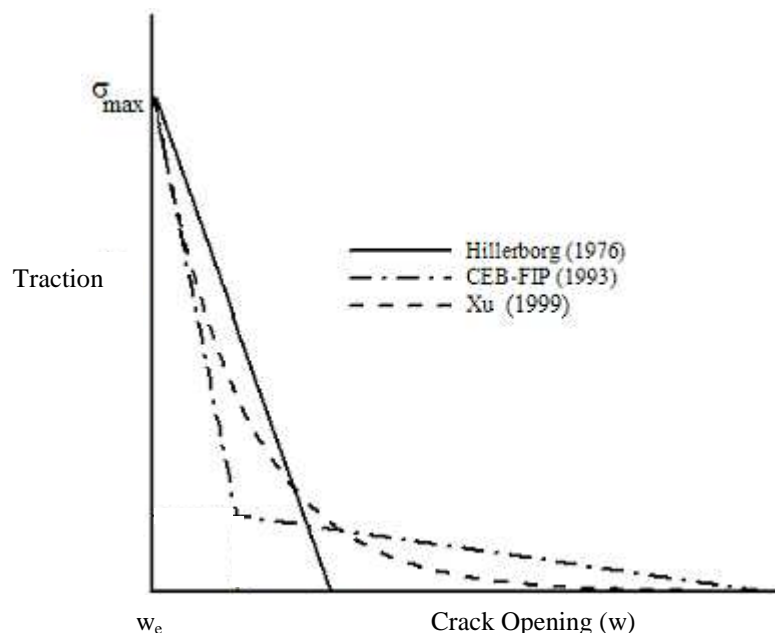
Figure 1: Post-peak cohesive traction (normal traction σ versus normal opening w) for pure Mode I.

The shape of post-peak traction-opening seems to be linked with the development of the so called process zone where many complex phenomena occur such as micro-cracking, interlock bridging, friction between surfaces and agregates, etc. The area under the curve is considered

the Mode I fracture energy (G_{IC}) and the maximal traction (σ_{max}) is related to the tensile strength. The shape of post-peak has an important influence on results (such as the maximum load achieved), as seen in Lens et al (2006). There are some practical indications that this curve should be steeper for smaller openings, due to intense micro-cracking, and much less steep for large openings due to bridging or interlock effects (Rots, 1988).

According to Xu (1999), G_{IC} depends mostly on f_{cm} and d_{max}. (f_{cm} is the average compression strength; f_{cm} - 8 MPa = f_{ck}, where f_{ck} is the characteristic compressive strength; d_{max} is the maximum aggregate diameter of the concrete). Then, when experimental information about fracture energy is not available, G_{IC} can be determined by equation (1) as follows (see Xu,1999)

$$G_{IC} = 0.0204 + 0.0056 \frac{d_{max}^{0.95}}{8}\left(\frac{f_{cm}}{10}\right)^{0.7} \tag{1}$$

where d_{max} is in mm and f_{cm} is in MPa. Based on previous studies (Lens et al., 2007), σ_{max} should range from 1 to 3 times the average tensile strength of the concrete, f_{tm}. Actually this range was also used by Carpinteri et al. (2003). According to these authors the relation σ_{max} x f_{tm}, depend on the size of the body ($\sigma_{max} = f_{tm}$ for large specimens and $\sigma_{max} = 3$ x f_{tm} for small specimens).

2.2 Pre-peak of the Constitutive Law

In the curves showed in Figure 1, the pre-peak portion is not depicted (crack opening from zero to w_e). This part of the curve is a non-dissipative elastic part of the surface opening. According to Rots (1988), w_e should be a small value in order that the elastic deformation of the cohesive surface is negligible compared to continuum elastic deformation. More important, we believe w_e should be a size dependent dimension, in order to avoid the introduction of an undesirable size effect. We propose here that,

$$w_e = \alpha \frac{\sigma_{max}}{E} l_c \tag{2}$$

where σ_{max}/E is the elastic deformation of the continuum at the peak load (in Mode I) and l_c is its characteristic length. α should be a small value (in general $\alpha << 1$). In a FE context, l_c is taken as the characteristic length of the FE at the fracture zone. The use of a constant w_e value would introduce an undesirable mesh dependence on results when cohesive surfaces are used between all FE. In a successive remeshing process, the sum of all w_e can be greater than the elastic volumetric displacements, which does not make sense. This effect can lead to a fake brittle (rather than quasi-brittle) behavior.

3   MIXED FRACTURE MODE

3.1 Preliminary Considerations

Damage curves for pure Mode II, tangential traction (τ) versus sliding (v), can be also defined, although experimentally difficult to obtain. Mode II energy (G_{IIC}) is then the area under the curve. The drop of normal (see Figure 1) and tangential tractions after peak, in the presence of a mixed mode, must be a function of a combination of both normal opening and sliding, through an effective opening. It can be defined as:

$$u_{eff} = \sqrt{w^2 + \beta v^2} \tag{3}$$

β ranges from 0 to 1. If no other coupling is introduced between Mode I and II, admissible space for tractions, when concrete is damaged by the rupture process, shrinks according to Figure 2 (τ_{max} represents maximal pure tangential traction, without damage).
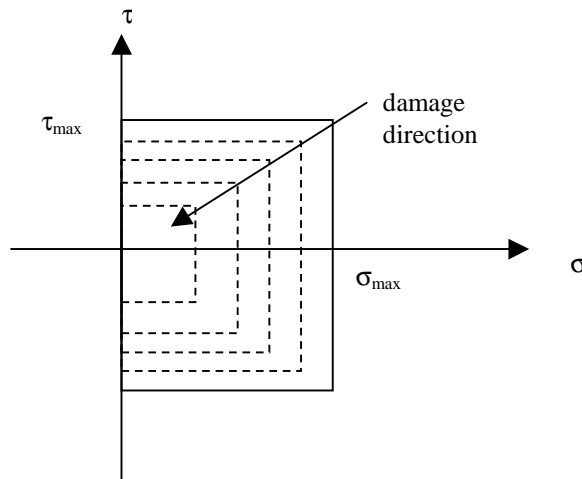
Figure 2: Evolution of traction space under tension.

Increasing damage, admissible region for tractions decreases, until it becomes a point at the origin of traction space. This point corresponds to fracture. The surfaces represented above can be also seen as an yield/cracking surface and analogies with plasticity can be built. According to the postulate of convexity of Drucker, the surfaces above can be seen as an upper bound limit in tension for a concrete cracking surface. A lower bound in tension is defined by the Coulomb´s law with adherence, being adherence initially σ_{max}. This case is depicted in Figure 3.
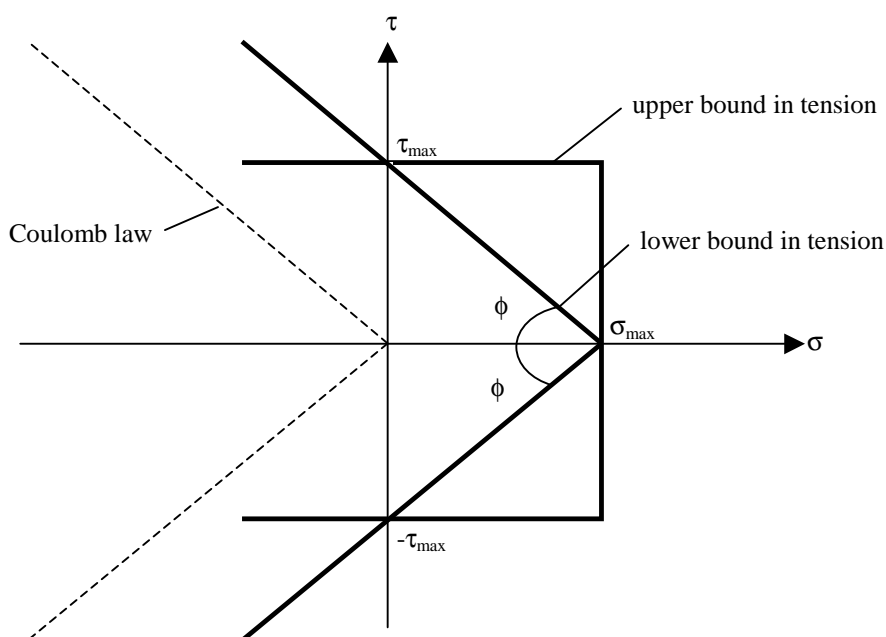
Figure 3: Possible cracking surfaces.

Besides giving a lower bound to cracking surface in tension, the use of Coulomb's law permits to have a model to deal with compressive normal tractions, as pointed out by Gálvez et al. (2002). In this case, shear resistance increases with compression, as expected. Considering total rupture (see Figure 3), original Coulomb's law is retrieved, meaning that tangential resistance is only possible under compression. Friction angle ϕ permits to determine maximal shear traction in pure Mode II (τ_{max}), once maximal normal traction in pure Mode I (σ_{max}) is known. Experiments indicate that this angle must be greater than 45°.

3.2 Modified Coulomb's Law

Yield/cracking surface F in this case is defined as

$$F = |\tau| + tan\,\phi\left(\sigma - f_t\right) = 0 \tag{4}$$

where $f_t = \sigma_{max}$ for undamage concrete (updating process for f_t is discussed below). For $F<0$ tractions are elastic and for $F=0$ damage or cracking is occurring.

In cases where F>0, stresses must return to the surface. An elastic-predictor, plastic-corrector type of algorithm is used. Elastic-predictor is given by equations (5) and (6).

$$\sigma^{el} = K_n w \tag{5}$$

$$\tau^{el} = K_t v \tag{6}$$

where K_n and K_t are the normal and tangential elastic stiffness of the interface, respectively. Their values are defined below:

$$K_n = \frac{\sigma_{max}}{w_e} \tag{7}$$

$$K_t = \frac{\tau_{max}}{v_e} \tag{8}$$

where, v_e is the tangential elastic opening. As its normal counterpart (equation 2), it is also a function of the characteristic length of the mesh l_c and α:

$$v_e = \alpha \frac{\tau_{max}}{\mu} l_c \tag{9}$$

μ is the concrete shear modulus. Incremantally, v and w can be also divided in an elastic and an irreversible part. This can be written as:

$$\begin{Bmatrix} \dot{w} \\ \dot{v} \end{Bmatrix} = \begin{Bmatrix} \dot{w}_e \\ \dot{v}_e \end{Bmatrix} + \begin{Bmatrix} \dot{w}_i \\ \dot{v}_i \end{Bmatrix} \tag{10}$$

Plastic corrector can be written according to eq. (11):

$$\begin{Bmatrix} \sigma \\ \tau \end{Bmatrix} = \begin{Bmatrix} \sigma^{el} \\ \tau^{el} \end{Bmatrix} - \begin{Bmatrix} K_n \\ K_t \end{Bmatrix} \int_{\Delta t} \begin{Bmatrix} \dot{w}_i \\ \dot{v}_i \end{Bmatrix} dt \tag{11}$$

A non-associated plasticity will be used here, which means that irreversible displacements are not normal to cracking surface *F*. Instead they are normal to a modified cracking surface *F**. The irreversible displacements are calculated as follows:

$$\begin{Bmatrix} \dot{w}_i \\ \dot{v}_i \end{Bmatrix} = \dot{\lambda} \begin{Bmatrix} \partial F^* / \partial \sigma \\ \partial F^* / \partial \tau \end{Bmatrix} \quad (12)$$

F* is seen in Figure 4, compared to *F*, and has two parts.
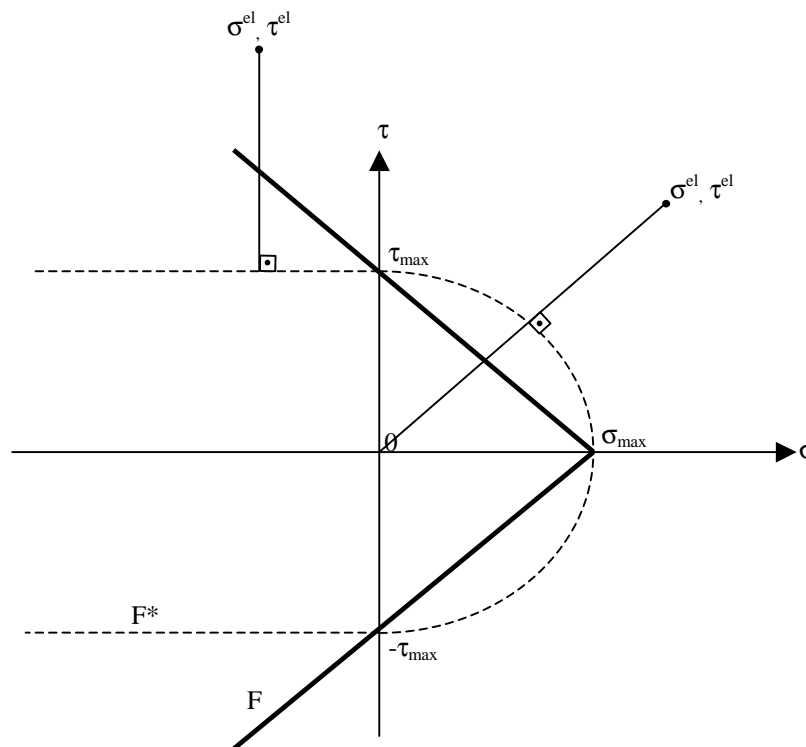
Figure 4: Cracking surface F and modified cracking surface F*.

For compressive normal tractions, only slidings are considered dissipative ($w_i = 0$), which is the usual hypothesis for friction (see for instance Bittencourt and Creus, 1998). In concrete, this hypothesis is valid only microscopically because, macroscopically, due to irregularities on crack surfaces, normal dissipative displacements will also occur (this effect is sometimes referred as dilatancy). For tensile normal tractions, dissipative displacements will be assumed to occur in the direction of the origin of the stress space. This assumption was also used by Gálvez et al. (2002) with good results.

Directions of irreversible displacements will be considered constant during integration process, so final stresses can be calculated as:

$$\begin{Bmatrix} \sigma \\ \tau \end{Bmatrix} = \begin{Bmatrix} \sigma^{el} \\ \tau^{el} \end{Bmatrix} - \begin{Bmatrix} K_n \\ K_t \end{Bmatrix} \begin{Bmatrix} \partial F^* / \partial \sigma \\ \partial F^* / \partial \tau \end{Bmatrix} \Lambda \quad (13)$$

where

$$\Lambda = \int_{\Delta t} \dot{\lambda} dt \quad (14)$$

The value of Λ can be obtained replacing eq. (13) into (4). Dissipative displacements w_i and v_i can be calculated from:

$$\begin{Bmatrix} w_i \\ v_i \end{Bmatrix} = \begin{Bmatrix} \partial F^* / \partial \sigma \\ \partial F^* / \partial \tau \end{Bmatrix} \Lambda \qquad (15)$$

and tractions updated from equation (13).
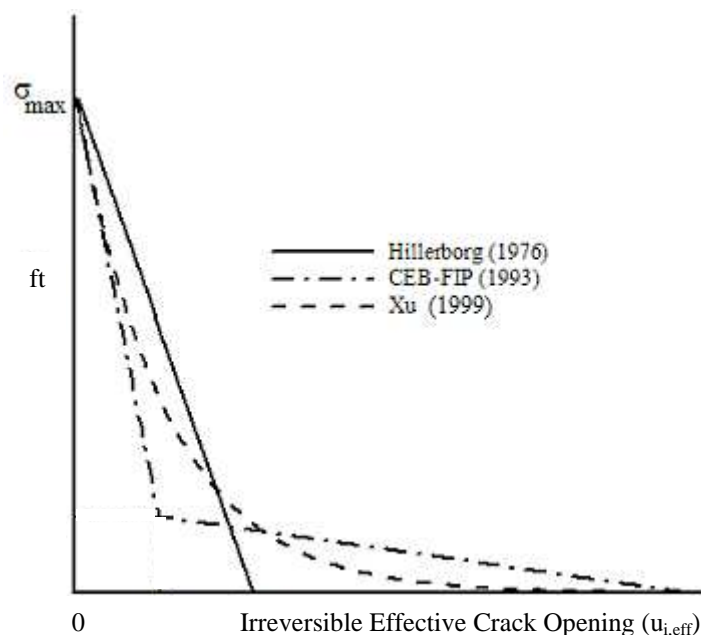
Figure 5: Post-peak normal cohesive traction as function of the irreversible effective crack opening.

As dissipative damage occurs, f_t must be also updated. This is done using the curves defined in Figure 5. Actually the procedure is the same used to update σ in pure Mode I (Figure 1), except that , w is replaced by the irreversible effective crack opening $u_{i,eff}$, as defined below.

$$u_{i,eff} = \sqrt{w_i^2 + \beta v_i^2} \qquad (18)$$

Finally, it can be seen that Mode II energy does not enter explicitly on the formulation, but indirectly through shear peak stress τ_{max} and β. For instance, if peak stress for Mode I and Mode II are the same, in this case G_{IIC} will be always greater than or equal to G_{IC}: for $\beta=1$, $G_{IIC}=G_{IC}$; for $\beta=0$, $G_{IIC}=\infty$.

4 NUMERICAL EXPERIMENTATION

4.1 Pure Mode I Propagation

In this section a three-point bending test is used to verify the behavior of the methodology in pure Mode I. The size and boundary conditions are defined in the Figure 6. Concrete properties are: Young modulus $E=23340$ MPa, $f_{ck}=25.2$ MPa and Poisson coefficient $v=0.20$. Cohesive surface properties are $G_{IC}=100$ N/m, $\sigma_{max}=1.8$ MPa and $\alpha=0.333$. The post-peak part of cohesive surface constitutive law does have an important effect not only in the post-peak behavior of the load x crack opening curve but also on the peak load itself. In all cases,

Hilleborg et al. (1976) induce a somewhat more brittle behavior, with greater peak load and more abrupt drop overall (see Figure 7).
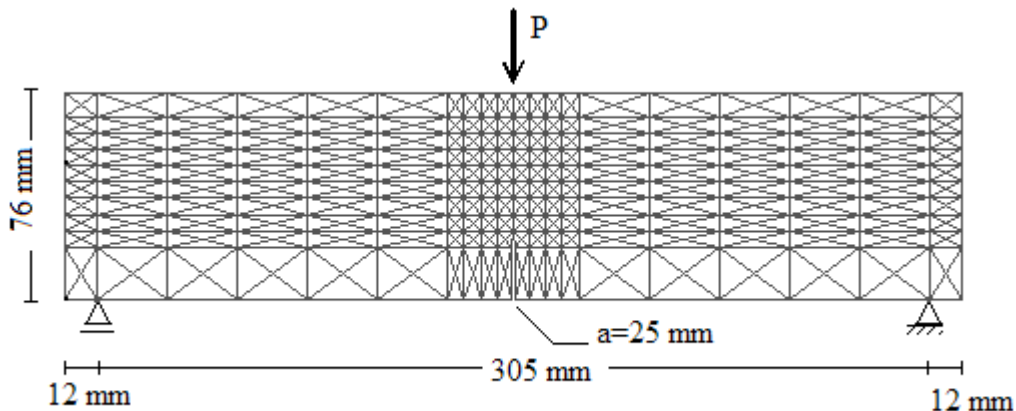
Figure 6: Geometry and boundary conditions.

The more brittle behavior induced by Hilleborg et al. (1976) when compared to experiments, can be associated to the absence of energy fracture for large openings, when bridging and interlock play an important effect. The CEB-FIP Model Code (1990) and Xu (1999) present a greater toughness, especially at large openings. In general Xu's constitutive law fits better experimental results.
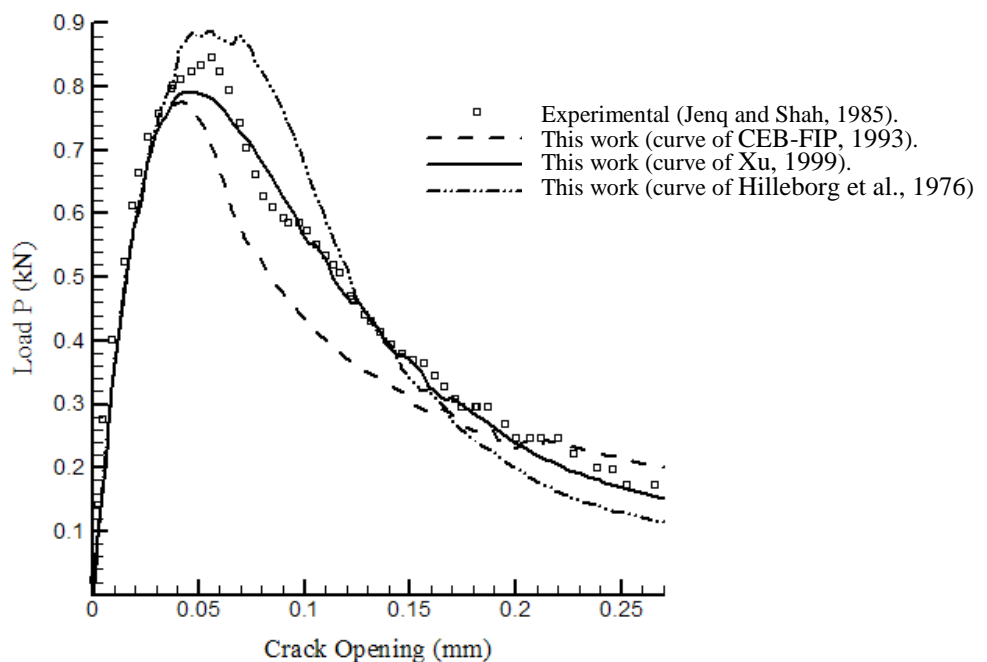
Figure 7: Various post-peak behaviors compared

Effects of the FE mesh was analyzed by the present authors for this case in Lens et al. (2007). It was shown that the present methodology has a smaller mesh dependency than classical cohesive surface methods.

4.2 Mixed Mode Propagation

To test the formulation in mixed mode propagation, a four-point double-notched shear beam, analyzed experimentally by Bocca et al. (1990), was here used. The FE mesh used and dimensions is depicted in Figure 8. Prescribed displacements are applied as indicated (application points are 20 mm apart from the beam center). Thickness is 100 mm. The Mode I energy was fixed in G_{IC}= 100 N/m. Mechanical properties are: Young modulus E=27000 MPa; Poisson coefficient ν=0.2.
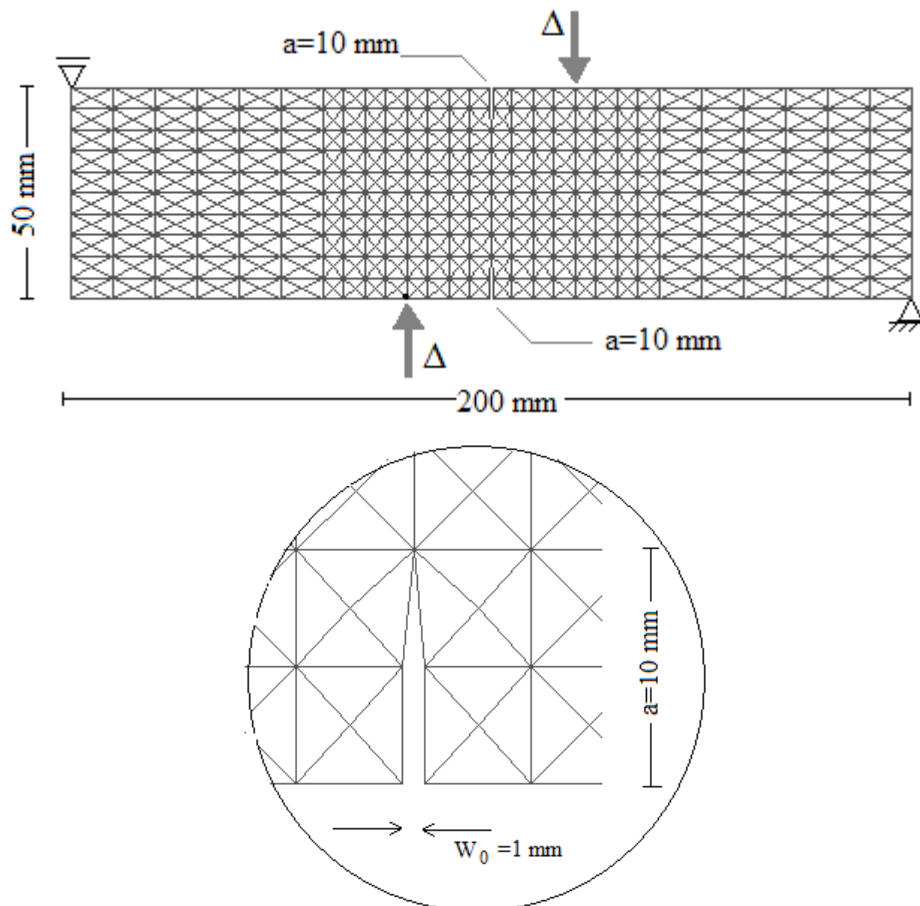
Figure 8: FE mesh with dimensions for the double-notched beam in mixed mode. Notch detail is also shown.

Figures 9a,b shows crack propagation at different moments of the cracking process (in this case σ_{max}=2.7 MPa; tan ϕ = 3.33; β = 1) and Figure 9c shows experimental fracture trajectory after total rupture of the beam. It can be noticed a remarkable similarity between numerical and experimental trajectory, with cracks changing trajectory at the beam edges. It is interesting to note that crack morphology was captured even with the coarse mesh used.

(a)

(b)

(c)
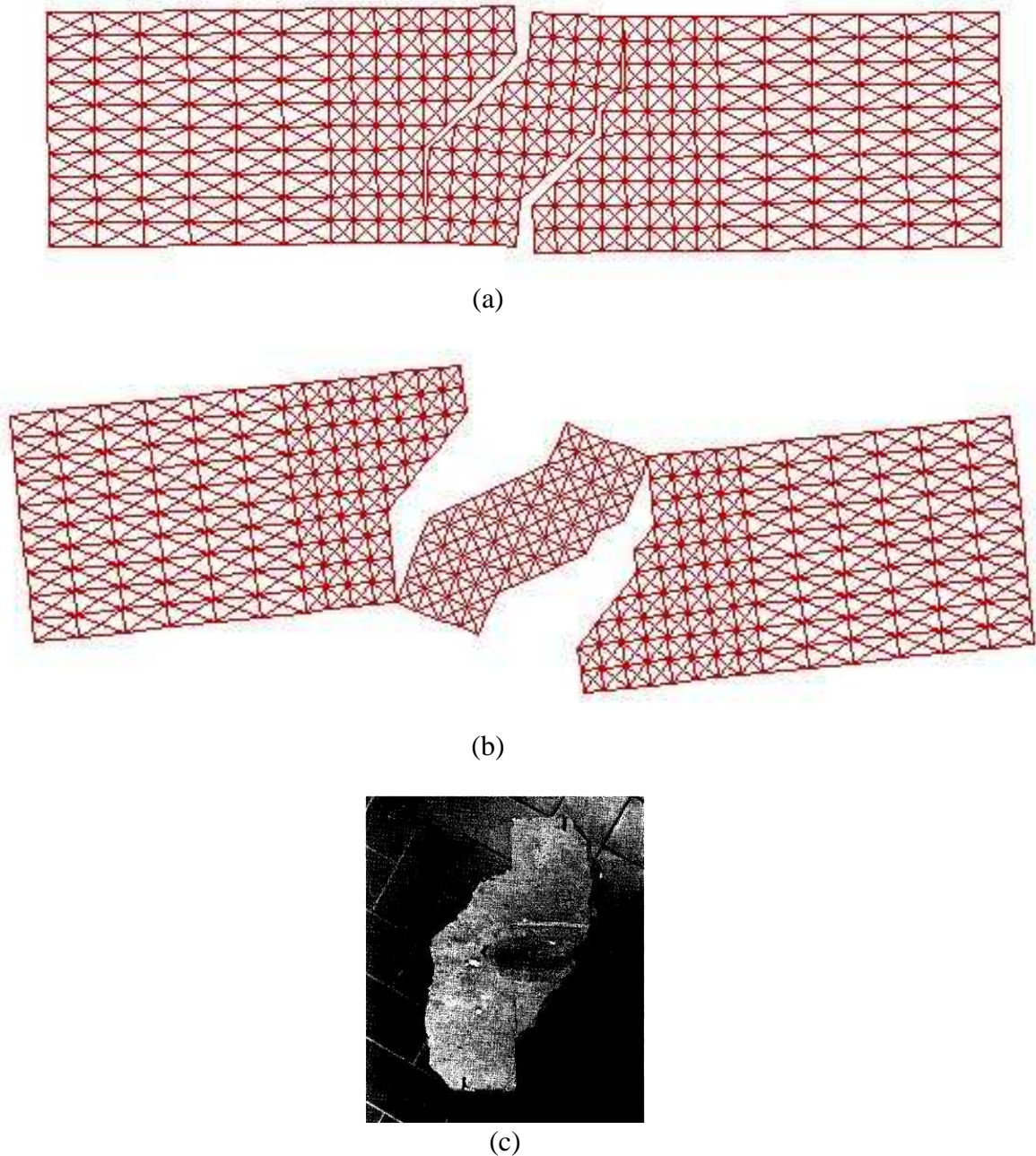
Figure 9: Crack trajectory at the beginning of propagation (a), at the final stage (b) and central part of the experimental beam after rupture (Bocca et al., 1990) (c) .

Figure 10 shows a plot of applied load (at the displacement points – see Figure 8) versus corresponding displacement for different Mode II properties (tan ϕ and β) with fixed Mode I properties (G_{IC} = 100N/m, σ_{max}=2.7 MPa). A peak load ranging from 11.8 to 12.4 KN was obtained, in very good agreement with the experimental result (12.2 KN). It is remarkable that Mode II properties have very little influence on results. On the other side, increasing maximal cohesion in Mode I (σ_{max}) to 3.7 MPa a significant increase in the peak load was observed (16.0 KN). Then it can be concluded that only pure Mode I properties need to be known to provide a good fitting with experiments. This trend was also observed by Bocca et al. (1990), Gálvez et al. (2002), among others.
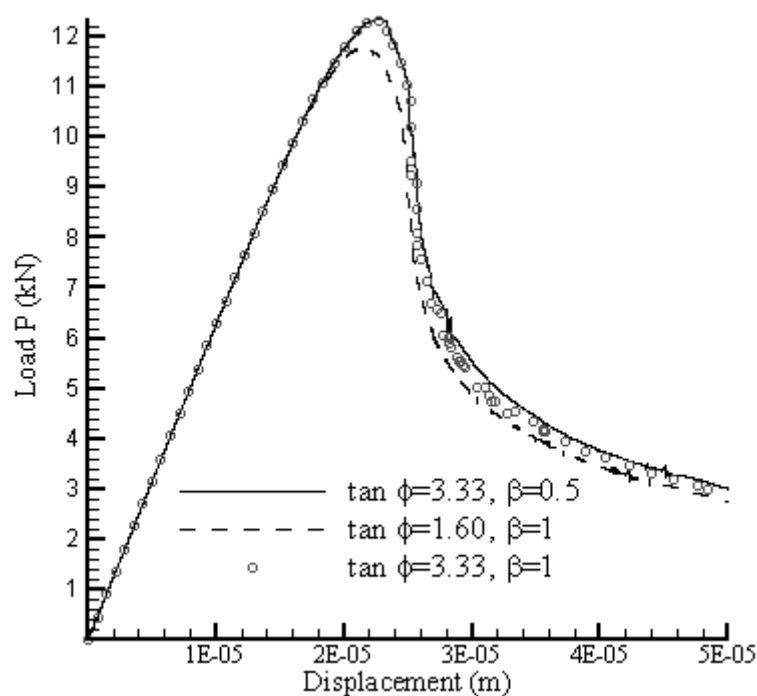
Figure 10: Influence of Mode II properties on load – displacement curve (σ_{max}=2.7 MPa; G_{IC}=100 N/m).

5 CONCLUSIONS

In this paper, a new formulation to deal with mixed mode fracture in plain concrete is presented. The model is based on a modified Coulomb's law. Comparing with pure Mode I algorithm, two new parameters need to be known: friction angle (or cohesion in pure Mode II) and a coupling factor.

In an exploratory example of a four-point double-notched beam, it was observed that properties necessary to consider Mode II practically do not change results. It was observed also that Mode I properties are determinant to define peak load and post-peak behavior. A coarse mesh was used and even in this case, the algorithm was able to reproduce crack trajectory with remarkable details. Tests with more refined meshes need to be done to confirm this trend.

REFERENCES

Basche, H. D., Rhee, I., William, K. J. and Shing, P. B. Analysis of shear capacity of lightweight concrete beams. *Engineering Fracture Mechanics*, 74:179-193, 2007.

Bazant, Z.P. and Cedolin, L., Blunt Crack Band Propagation in Finite Element Analysis. *Journal of the Engineering Mechanics Division*, *ASCE*, 105:297-315, 1979.

Belytschko, T., Fish, J. and Engelmann, B.E., A Finite Element with Embedded Localization Zones. *Computer Methods in Applied Mechanics and Engineering*, 70:59-89, 1988.

Belytschko, T. and Black, T., Elastic Crack Growth in Finite Elements with Minimal Remeshing. *International Journal for Numerical Methods in Engineering*, 45:601-620, 1999.

Belytschko, T., Moes, N., Usui, S. and Parimi, C., Arbitrary Discontinuities in Finite Elements. *International Journal for Numerical Methods in Engineering*, 50:993-1013, 2001.

Bittencourt, E. and Creus, G. J., Finite Element analysis of three-dimensional contact and impact in large deformation problems, *Computers and Structures*, 69:219-234, 1998

Bocca, P., Carpinteri, A. and Valente, S., Size Effects in the Mixed Mode Crack Propagation: Softening and Snap-back Analysis. *Engineering Fracture Mechanics*, 35:159-170, 1990.

Brisotto, D. S., d´Avila, V. M. R and Bittencourt, E., Numerical simulation of cracking in reinforced concrete members by an embedded model. *Engineering Computations*, in press, 2008.

Camacho, G. T. and Ortiz, M., Computational modelling of impact damage in brittle materials. *International Journal of Solids and Structures*, 33:2899-2938, 1996.

Carpinteri, A., Valente, S., Ferrar, G. and Melchiorri, G., Is mode II fracture energy a real material property?. *Computers and Structure,* 48:397–413, 1993.

Carpinteri, A., Cornetti, P., Barpi, F. and Valente, S. Cohesive crack model description of ductile to brittle size-scale transition: dimensional analysis vs. renormalization group theory. *Engineering Fracture Mechanics*, 70:1809-1839, 2003.

CEB-FIP Model Code 1990 - Comité Euro-International du Béton. *Bulletin d'Infornacion*, Lausance, 213/214, 1993.

Cedolin, L.; and dei Poli, S. Finite Element Studies of Shear-Critical R/C Beams. *Journal of Engineering Mechanics Division*, *ASCE*, 103:395-410, 1977.

Cervenka, J., *Discrete crack modeling in concrete structures*. PhD. Thesis, University of Colorado, Boulder, 1994.

Chandra, N., Li, H., Shet, C. and Ghonem, H. Some issues in the application of cohesive zone models for metal-ceramic interfaces. *International Journal of Solids and Structures*, 39:2827-2855, 2002.

di Prisco, M., Ferrara, L., Meftah, F., Pamin, J., de Borst, R., Mazars, J. and Reynouard, J. Mixed mode fracture in plain and reinforced concrete: some results on benchmark tests, *International Journal of Fracture,* 103:127–148, 2000.

Dominguez, N., Brancherie, D., Davenne, L. and Ibrahimbegovic, A. Prediction of crack pattern distribution in reinforced concrete by coupling a strong discontinuity model of concrete cracking and a bond-slip of reinforcement model. *Engineering Computations*, 22:558-582, 2004.

Dvorkin, E.N., Cuitiño, A.M. and Gioia, G. Finite Elements with Displacement Interpoled Embedded Localization Lines Insensitive to Mesh Size and Distortions. *International Journal for Numerical Methods in Engineering*, 30:541-564, 1990.

Gálvez, J.C., Cervenka, J., Cendón, D.A. and Saouma, V. A Discrete Crack Approach to Normal/shear Craking of Concrete. *Cement and Concrete Research - ASCE*, 32:1567-1585, 2002.

García, V.O, Gettu, R. and Carol, I. Numerical analysis of mixed mode fracture in concrete using interface elements. *European Congress on Computational Methods in Applied Sciences and Engineering*, Barcelona, Spain, 2000.

Grootenboer, H.J., Leijten, S.F.C.H. and Blaauwendrad, J. Numerical Models for Reinforced Concrete Structures in Plane Stress. *HERON*, 26:1C, 1981.

Gupta, A.K. and Maestrini, S.R. Unified Approach to Modeling Post-Cracking Membrane Behavior of Reinforced Concrete. *Journal of Structural Engineering*, *ASCE*, 115:977-993, 1989.

Gupta, A.K. and Maestrini, S.R. Tension-Stiffness Model for Reinforced Concrete Bars,

Journal of Structural Engineering - ASCE, 116:769-790, 1990.

Hilleborg, A. Modéer, M. and Peterson, P.E. Analysis of crack formation and crack growth in concrete by means of fracture mechanics and finite elements. *Cement and Concrete Research*, 6:773-782, 1976.

Jenq, Y.S. and Shah, S.P. A fracture toughness criterion for concrete. *Engineering Fracture Mechanics*, 21:1055-1069, 1985.

Jenq, Y. and Shah, S.P., Mixed-mode fracture of concrete. *International Journal of Fracture,* 38:123–142, 1988.

Lens, L.N., Bittencourt, E. and d'Avila, V.M.R. Cohesive Laws to Model Concrete Rupture - A Methodology that takes Mesh Effects into Consideration. *ENIEF*, Cordoba, Argentina, 2007.

Lens, L.N., Bittencourt, E. and d'Avila, V.M.R. Quasi-fragile and fragile fracture behavior with the cohesive surface methodology. *MECOM*, Santa Fé, Argentina, 2006.

Oliver, J. A "Consistent Characteristic Length for Smeared Cracking Models", International Journal for Numerical Methods in Engineering, 28:461-474, 1989.

Ortiz, M., Leroy, Y. and Needleman, A. A finite element method for localized failure analysis. *Computer Methods in Applied Mechanics and Engineering*, 61:189-214, 1987.

Potyondy, D. O., Wawrzynek, P. A. and Ingraffea, A. R. Element Surface Meshes in Arbitrary Domains with Applications to Crack-Propagation. *International Journal for Numerical Methods in Engineering*, 16:2677-2701, 1995.

Rashid, Y.R. Ultimate Strength Analysis of Prestressed Concrete Pressure Vessels. *Nuclear Engineering and Design*, 7:334-344, 1968.

Rots. J.G. *Computational modeling of concrete fracture*. PhD Thesis, Delft University, 1988.

Rots, J.G. and Blaauwendrad, J. Crack Models for Concrete: Discrete or Smeared? Fixed, Multi-directional or Rotating? *HERON*, 34, 1989.

Shah, S.P., Swartz, S.E. and Ouyang, C. *Fracture mechanics of concrete: applications of fracture mechanics to concrete, rock and other quasi-brittle material*. Wiley-Interscience publication, 1995.

Swartz, S.E., Lu, L., Tang, L. and Refai, T., Mode II fracture parameter estimates for concrete from beam specimens. *Experimental Mechanics*, 28:146–153, 1988.

Wawrzynek, P. A. and Ingraffea, A. R. Interactive Finite-element Analysis of Fracture Processes – An Integrated Appoach. *Theoretical and Applied Fracture Mechanics*, 8:130-150, 1987.

Xu, X.P. Determination of parameters in the bilinear, Reinhardt´s non-linear and exponentially non-linear softeming curves and their physical meanings. *Werkstoffe und Werkstoffprüfung im Bauwesen*, 410-424, 1999.

Xu, X.P. and Needleman, A. Numerical simulations of fast crack growth in brittle solids. *Journal Mech. Phys. Solids*, 42:1397-1424, 1994.